Zonal Multi-Layer Predictive Control for Multi-Conjugate Adaptive Optics: MAVIS Simulations

Jesse Cranney[a,b], Jose De Dona[a], Francois Rigaut[b,c], and Visa Korkiakoski[b,c]

[a]School of Electrical Engineering and Computing, University of Newcastle, Callaghan, Australia
[b]SERC Limited, Canberra, Australia
[c]Mt Stromlo Observatory, Australian National University, Canberra, Australia

ABSTRACT

MAVIS (MCAO-Assisted Visible Imager & Spectrograph) is a proposed instrument for ESO's VLT Adaptive Optics Facility. MAVIS aims at providing near-diffraction limited images across a 30" FoV. Predictive control allows an increased sky-coverage and is therefore attractive for use in the MAVIS application. This brief communication presents the problem statement, control law, estimation strategy, and simulations for one such scheme in the MAVIS context: a predictive zonal minimum-variance linear quadratic Gaussian controller based on the frozen-flow hypothesis.

Acknowledgments

The authors would like to acknowledge the support of the Cooperative Research Centre for Space Environment Management (SERC Limited) through the Australian Government's Cooperative Research Centre Programme.

1. INTRODUCTION

MAVIS (MCAO-Assisted Visible Imager & Spectrograph) is a proposed instrument for ESO's VLT Adaptive Optics Facility that will provide near-diffraction limited image quality over a large field of view using Multi-Conjugate Adaptive Optics [1]. Predictive control schemes in tomographic AO are expected to increase sky-coverage and overall performance [2], and therefore should be considered for the MAVIS application.

Here, one such predictive control scheme is considered. This scheme is implemented on a zonal basis using the minimum variance turbulence model under the thin-layer frozen flow assumption [3–5]. The turbulence is assumed to be Von Karman, with covariance given by [6]:

$$C(r) = \left(\frac{L_0}{r_0}\right)^{5/3} \frac{\Gamma(11/6)}{2^{5/6}\pi^{8/3}} \left[\frac{24}{5}\Gamma\left(\frac{6}{5}\right)\right]^{5/6} \left(\frac{2\pi r}{L_{0,\ell}}\right)^{5/6} K_{5/6}\left(\frac{2\pi r}{L_0}\right) \tag{1}$$

The turbulence is modeled as L layers, sampled spatially on independent square grids for each layer, with these samples being vertically concatenated to form the complete state vector, $\phi(t)$. This continuous-time state is time-averaged over one sampling period T to give the discrete-time state vector [7]:

$$\phi_k \triangleq \frac{1}{T}\int_{(k-1)T}^{kT} \phi(t)\,\mathrm{d}t$$

The model for the turbulence evolution is then:

$$\phi_{k+1} = A\phi_k + v_k \tag{2}$$

Further author information (for correspondence):
Jesse Cranney: E-mail: jesse.cranney@uon.edu.au, Telephone: +61 403 144 392

where v_k is additive white process noise with covariance given by $\langle v_k v_k^\mathsf{T} \rangle$ ($\langle x \rangle$ denotes the expected value of the random variable x), and A is given by [3]:

$$A = \langle \phi_{k+1} \phi_k^\mathsf{T} \rangle \langle \phi_k \phi_k^\mathsf{T} \rangle^{-1} \tag{3}$$

This choice of A matrix is able to model the dynamics of the evolving turbulence due to wind shifts (under the frozen flow assumption) so long as the speed and direction of wind is known for each layer a priori. Eqns (2) & (3) give a closed-form expression for the process noise covariance matrix so long as the model of the turbulence evolution is not time-varying (i.e. it has stationary statistics) and ϕ_k and v_k are uncorrelated:

$$\langle v_k v_k^\mathsf{T} \rangle = \langle \phi_k \phi_k^\mathsf{T} \rangle - A \langle \phi_k \phi_k^\mathsf{T} \rangle A^\mathsf{T}$$

$\langle \phi_{k+1} \phi_k^\mathsf{T} \rangle$ and $\langle \phi_k \phi_k^\mathsf{T} \rangle$ can be found from Eqn (1). The measurement of the AO loop is performed by an array of Shack-Hartmann WFS (SHWFS), one for each guide star. The output equation can be linearly modeled using *ray-tracing* under the near-field approximation to project the turbulence phase in each layer, and the phase contributed by each deformable mirror (DM), into the WFS slope space [2, 8]. The linear output equation is:

$$s_k = C\phi_{k-1} + Du_{k-2} + w_k$$

where C and D are the projection matrices from turbulence→WFS and DM→WFS respectively, u_k is the command applied from time $t = [kT, (k+1)T)$ (assumed constant over this interval), and w_k is the measurement noise with covariance $\langle w_k w_k^\mathsf{T} \rangle$. The control law is a linear function of the estimated turbulence state given all presently available measurements:

$$u_k = K\hat{\phi}_{k|k} \tag{4}$$

where K is chosen such that u_k minimises a given performance objective. In the MCAO case, the goal is to minimise the residual wave-front uniformly over the entire field of view, so the cost function to regulate is the following quadratic expression [9]:

$$J_{u_k} = \lim_{N \to \infty} \sum_{i=1}^{N} \left\| \phi_{k+1}^{\text{tur},\alpha_i} - \phi_{k+1}^{\text{cor},\alpha_i} \right\|^2 \tag{5}$$

where $\phi^{\text{tur},\alpha}$ and $\phi^{\text{cor},\alpha}$ are the integrated phase in the direction α due to the turbulence and DM correcting phase respectively. The N directions, $\alpha_i,\ i \in [1, 2, \ldots, N]$, are chosen to be uniformly distributed across the field of view. To make the cost function have a computationally tractable solution, N is chosen to be a large finite integer, in which case a linear control law is able to be computed in the form of Eqn (4).

The estimation of the state ϕ_k is performed by the steady-state Kalman Filter. This is achieved using the recursion:

$$\hat{\phi}_{k|k} = (A - LC)\hat{\phi}_{k-1|k-1} + Ls_k - LDu_{k-2}$$

where L is the Kalman Gain, which is found by solving the Discrete Algebraic Riccati Equation (DARE) for P:

$$P = APA^\mathsf{T} + \langle v_k v_k^\mathsf{T} \rangle - APC^\mathsf{T} \left(\langle w_k w_k^\mathsf{T} \rangle + CPC^\mathsf{T} \right)^{-1} CPA^\mathsf{T}$$

and $L = APC^T \left(\langle w_k w_k^\mathsf{T} \rangle + CPC^\mathsf{T} \right)^{-1}$. Combining the Kalman Filter and the Linear Quadratic Regulator gives the Linear Quadratic Gaussian (LQG) control scheme with closed loop recursive equations:

$$\hat{\phi}_{k|k} = (A - LC)\hat{\phi}_{k-1|k-1} + Ls_k - LDu_{k-2} \tag{6}$$

$$u_k = K\hat{\phi}_{k|k} \tag{7}$$

2. SIMULATIONS

In this section we present a series of simulation studies for the MAVIS setup.

2.1 Varying the Number of Directions N

In the Full-Field Correction MCAO mode, a large number of directions (N) are chosen. As expected, the performance of the AO loop improves as this number increases, with diminishing improvements above some level.

Here, we examine the performance across the field of view as N grows. To do this, we require a method of uniformly distributing the directions of observation over a given disk. We choose to do this by utilising the *golden angle*, g, which uniformly distributes points across a disk:

$$g = (3 - \sqrt{5})\pi \text{ rad}$$

and the distribution of our m points across the field of view is given by:

$$\alpha_i^x = R_{\text{FoV}} \sqrt{\frac{i}{N}} \cos(i \cdot g) \tag{8}$$

$$\alpha_i^y = R_{\text{FoV}} \sqrt{\frac{i}{N}} \sin(i \cdot g) \tag{9}$$

for $i = 1, 2, \ldots, N$, where R_{FoV} is the radius of the field of view of the science field. Figure 1 shows the distribution of points according to this function for particular values of N.

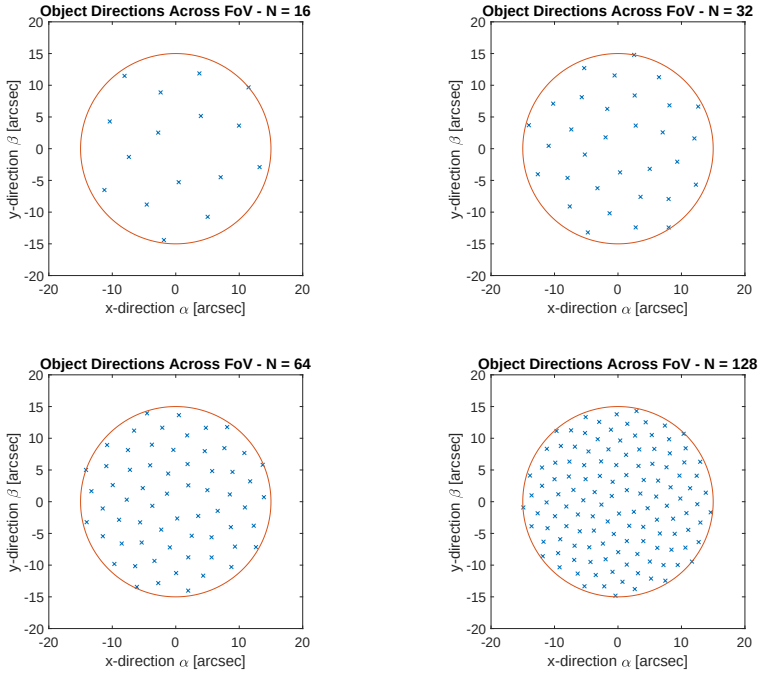

Figure 1. Object Directions for MCAO Full Field Correction using the *golden angle* to distribute N directions uniformly.

The simulation parameters are based on the MAVIS project*, and are summarised in Table 1. The results

*All guide-stars used here are NGS, as opposed to the planned MAVIS operation, which is expected to be a combination of NGS for low order correction and LGS for high order correction. A complete study of the performance under different guide-star configurations for predictive control in MAVIS is still required and will be investigated in future research.

Table 1. Simulation Parameters Based on MAVIS

Parameter	Value
# WFS	6
#subapertures/WFS	40×40 (1240 active)
# DM	3 (piezoelectric stack)
#actuators/DM	41×41 ([1313, 1045, 999] active)
# DM altitudes	$[0, 4, 12]$km
guide star position	$17''\angle 60n,\ n \in [1, \ldots, 6]$
target FoV	$14''$
wavelength λ	650nm
Fried parameter r_0	0.13m
diameter	8m
control period T	2ms
control delay	2 frames
GS Flux	187-320 photons/subap/frame
turbulence altitudes	$[0, 3, 6, 13]$km
turbulence wind-speed	$[15\angle 0°, 20\angle 60°, 25\angle 120°, 20\angle 180°]$m/s
turbulence weight	$[0.4, 0.3, 0.2, 0.1]$

shown in Figure 2 demonstrate the change in performance as N is increased for a fixed FoV of $15''$. The

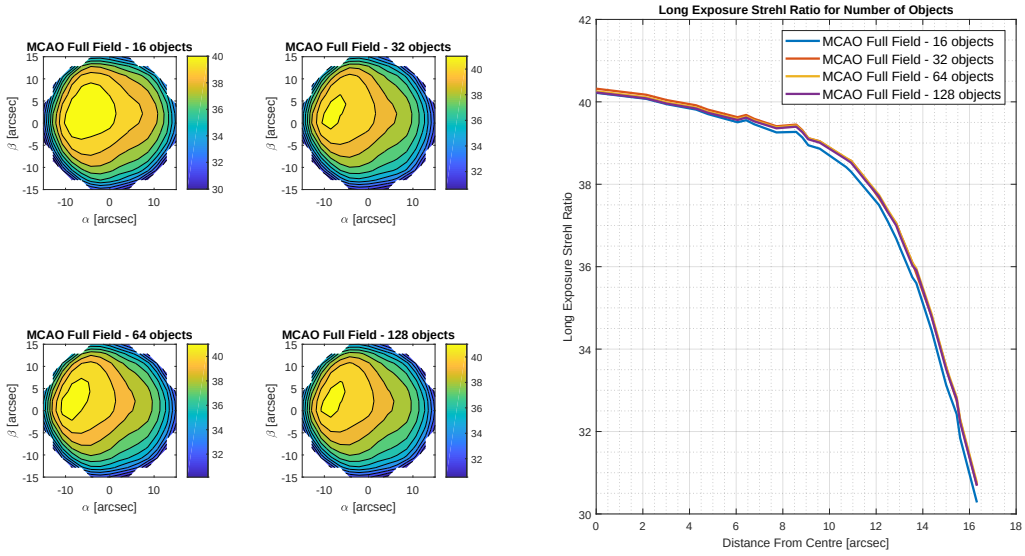

Figure 2. Long Exposure SR. MCAO attempting full field correction for various numbers of target objects

performance is marginally higher as the number of directions increases. Note that the offline computational demand in computing K increases approximately linearly with the number of directions.

2.2 Varying SNR

The performance over a range of signal to noise ratios (SNRs) can be evaluated by varying the guide-star flux and keeping the integration time/control period constant. As can be seen in Figure 3, the long exposure Strehl Ratio (SR) over the entire FoV decreases as the WFS noise becomes dominant. Figure 4 shows the average long exposure SR over the entire field of view as the NGS flux changes. *MLPC* refers to the control scheme discussed

in this paper and the non-predictive gain optimised *MMSE* controller is shown for comparison [9]. Performance is relatively constant above 200 photons/sub-aperture/sample, and degrades for fluxes lower than this until the noise becomes insurmountable (around 10 photons/subaperture/sample for both MLPC and MMSE).

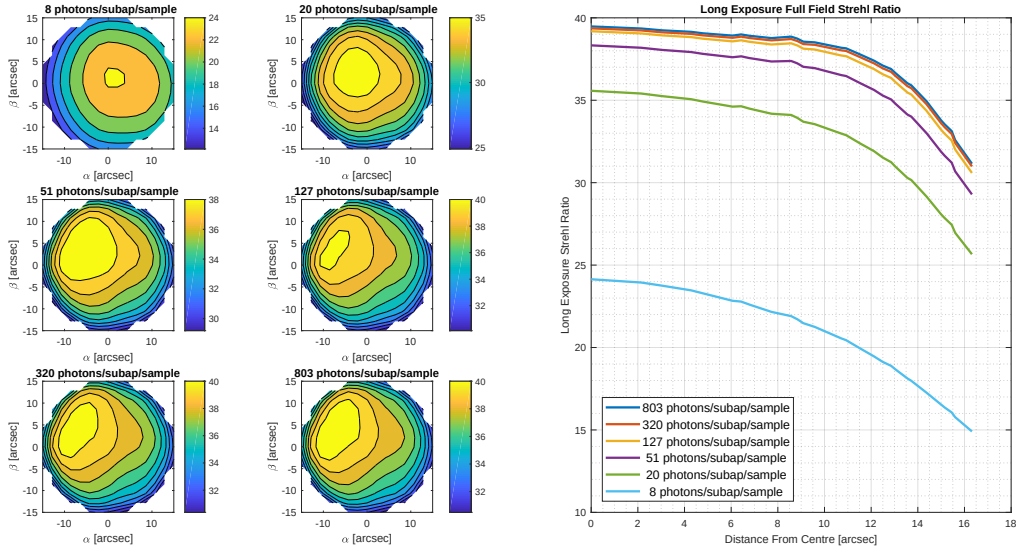

Figure 3. Long Exposure SR. MCAO attempting full field correction for different guide-star fluxes

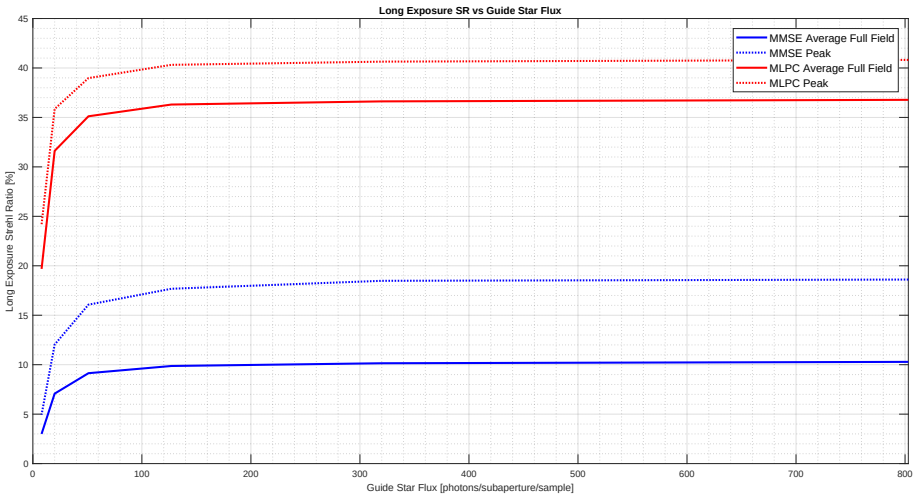

Figure 4. Wide field average long exposure SR as a function of guide-star flux

3. CONCLUSION

The zonal multi-layer predictive control scheme for MCAO appears to be suitable for the MAVIS application. Wide-field long-exposure Strehl ratios in excess of more than 30% at 650nm were achieved in simulation across

the entire 30" FoV for the high flux NGS case. Further studies into the guide-star configuration and different DM configurations are required, as well as comparisons of this method with other state-of-the-art control techniques.

References

[1] Rigaut. F. *About MAVIS*. 2019. URL: http://mavis-ao.org/mavis/.

[2] C. Correia et al. "Static and predictive tomographic reconstruction for wide-field multi-object adaptive optics systems". In: *J. Opt. Soc. Am. A 31, 101-113* (2014).

[3] D. T. Gavel and D. M. Wiberg. "Towards Strehl-optimizing adaptive optics controllers". In: *Proc. SPIE 4839, 972-982* (2002).

[4] P. Piatrou and M. Roggermann. "Performance study of Kalman filter controller for multiconjugate adaptive optics." In: *Applied Optics, 46(9):1446-55.* (2007).

[5] L. Poyneer, M. van Dam, and J. P. Véran. "Experimental verification of the frozen flow atmospheric turbulence assumption with use of astronomical adaptive optics telemetry". In: *J. Opt. Soc. Am. A. Vol. 26, No. 4,* (2009).

[6] Assemat. F, Wilson. R, and Gendron. E. "Method for simulating infinitely long and non stationary phase screens with optimized memory storage". In: *Opt. Express 14, 988-999* (2007).

[7] Caroline Kulcsár et al. "Optimal control, observers and integrators in adaptive optics". In: *Opt. Express 14, 7464-7476* (2006).

[8] C. Petit et al. "LQG control for adaptive optics and multiconjugate adaptive optics: experimental and numerical analysis," in: *J. Opt. Soc. Am. A 26, 1307-1325* (2009).

[9] B. Le Roux, J.M. Conan, and et al. C. Kulcsár. "Optimal control law for classical and multiconjugate adaptive optics," in: *J. Opt. Soc. Am. A 21, 1261-1276* (2004).